

Geophysical Research Letters

RESEARCH LETTER

10.1029/2020GL088288

Key Points:

- Damming decouples the global river fluxes of N, P, and Si
- Dams increase N:P ratios delivered to the global coastal zone
- Current hydroelectric dam construction may drive coastal productivity toward increased Si limitation

Supporting Information:

- Supporting Information S1

Correspondence to:

T. Maavara,
taylor.maavara@yale.edu

Citation:

Maavara, T., Akbarzadeh, Z., & Van Cappellen, P. (2020). Global dam-driven changes to riverine N:P:Si ratios delivered to the coastal ocean. *Geophysical Research Letters*, 47, e2020GL088288. <https://doi.org/10.1029/2020GL088288>

Received 4 APR 2020

Accepted 13 JUL 2020

Accepted article online 17 JUL 2020

Global Dam-Driven Changes to Riverine N:P:Si Ratios Delivered to the Coastal Ocean

Taylor Maavara¹ , Zahra Akbarzadeh² , and Philippe Van Cappellen²

¹School of the Environment, Yale University, New Haven, CT, USA, ²Ecohydrology Research Group, Water Institute, and Department of Earth and Environmental Sciences, University of Waterloo, Waterloo, Ontario, Canada

Abstract River damming alters nutrient fluxes along the land-ocean aquatic continuum as a result of biogeochemical processes in reservoirs. Both the changes in riverine nutrient fluxes and nutrient ratios impact ecosystem functioning of receiving water bodies. We utilize spatially distributed mechanistic models of nitrogen (N), phosphorus (P), and silicon (Si) cycling in reservoirs to quantify changes in nutrient stoichiometry of river discharge to coastal waters. The results demonstrate that the growing number of dams decouples the riverine fluxes of N, P, and Si. Worldwide, preferential removal of P over N in reservoirs increases N:P ratios delivered to the ocean, raising the potential for P limitation of coastal productivity. By midcentury, more than half of the rivers discharging to the coastal zone will experience a higher removal of reactive Si relative to reactive P and total N, in response to the rapid pace at which new hydroelectric dams are being built.

Plain Language Summary The damming of rivers is one of the most impactful modifications of the flows of water and associated materials from land to sea. Included in these materials are nutrient elements like nitrogen and phosphorus, which are elements required by all life on Earth, and silicon, which is required by diatoms, the algae that account for the largest fraction of biological productivity of the oceans. Past studies have shown that if you alter the ratios in which these nutrient elements enter the coastal oceans, plankton communities can change, even causing harmful algal blooms or “red tides” to occur. Here, we use models of nitrogen, phosphorus, and silicon cycling in dam reservoirs to determine how dams change the ratios delivered to coastal zones worldwide. We predict that by midcentury, more than half of the rivers flowing to the sea will experience greater removal of silicon over nitrogen and phosphorus, in response to ongoing construction of many new hydroelectric dams. This will impact the role of diatoms in nearshore marine production, as they are increasingly outcompeted by other, potentially harmful, algae that do not need silicon to grow.

1. Introduction

Human activities have altered the absolute and relative magnitudes of riverine nutrient fluxes. Changes in riverine nutrient stoichiometry may alter the structure and functioning of downstream coastal ecosystems by modifying which macronutrient element(s) controls primary productivity (Royer, 2020). Nitrogen (N) and phosphorus (P) loads to coastal zones have at least doubled since preindustrial times (Compton et al., 2000; Filippelli, 2008; Galloway et al., 2004; Vitousek et al., 1997), largely due to enhanced fertilizer application and wastewater discharge to rivers. In contrast to P and N, the global supply of the nutrient silicon (Si) to rivers has been reduced by human activities, including harvesting of Si-rich agricultural and forest products (Struyf et al., 2010; Vandevenne et al., 2012).

In coastal systems, nutrient ratios are typically benchmarked against the molar Redfield ratios C:N:P = 106:16:1, which describe the average elemental composition of soft-tissue phytoplankton (Redfield, 1934). The Redfield ratio concept has been expanded to describe Si uptake requirements of marine diatoms, yielding C:N:P:Si = 106:16:1:~15–20 (Brzezinski, 1985). Marine diatoms account for up to a quarter of global primary productivity and 40% of oceanic primary production (Buchan et al., 2014; Falkowski et al., 1998). The high fatty acid content of diatoms, up to 25% dry weight (Mangas-Sánchez & Adlercreutz, 2015), promotes high growth, survival, and reproductive rates in marine and freshwater ecosystems (Brett & Müller-Navarra, 1997), hence providing diatoms with a competitive advantage when sufficient Si is available.

Variations in nutrient stoichiometry can have multiple ecological impacts in the coastal zone. Long-term decreases in Si:P and Si:N ratios have been correlated with the decline of coastal diatom communities in, for instance, the Baltic Sea, East China Sea, and Seine and Scheldt estuaries (Billen & Garnier, 2007; Gong et al., 2006; Humborg et al., 2006; Officer & Ryther, 1980). Fewer diatoms in turn diverts more of the available N and P to nonsiliceous plankton that, in some cases, have been linked to the occurrence of nuisance and toxic algal blooms (Billen et al., 1991). A change in the relative availability of Si may also affect the structure of the siliceous plankton communities themselves. For example, in the Gulf of Mexico decreasing Si:N ratios in sediment cores dating back to 1950 correlate with the rise of the diatom genus *Pseudo-nitzschia*, which are lightly silicified and thus have a lower Si requirement than other diatom species. The enhanced occurrence of *Pseudo-nitzschia* has been attributed to decreases in the Si:N ratio of the Mississippi River discharge into the Gulf of Mexico (Parsons et al., 1999, 2002). Blooms of *Pseudo-nitzschia* are undesirable because some species produce the neurotoxin domoic acid (Bates et al., 2018).

River damming profoundly affects the freshwater cycle and nutrient fluxes along the aquatic continuum (Friedl & Wüest, 2002; Maavara et al., 2020; Maranger et al., 2018). We are now in the midst of the largest boom in dam construction since the 1950s to the 1970s (Lechner et al., 2011; Zarfl et al., 2015). Approximately 3,700 new large hydroelectric dams (classified as those with generating capacities ≥ 1 MW) are currently under construction or planned, effectively doubling the number of dams in this category (Zarfl et al., 2015). While at present, a third of large rivers ($>1,000$ km long) remain free flowing (Grill et al., 2019), by 2030 up to 93% of all river systems on Earth will be fragmented by dams (Grill et al., 2015). Damming lengthens hydraulic residence times (τ_r) along the aquatic continuum (Vorosmarty et al., 1997), driving the removal of nutrients from waterways via transformations into particulate forms, followed by sedimentation and burial, or via gaseous elimination.

River loads of N and P are augmented by anthropogenic sources, but Si loads are not, thus generally decreasing Si:N and Si:P ratios reaching coastal zones (Billen & Garnier, 2007; Garnier et al., 2010; Gong et al., 2006; Humborg et al., 2006; Strokal et al., 2014). In addition to differences in nutrient loads to rivers, dams further decouple global nutrient river fluxes because of variable removal efficiencies of nutrient elements in reservoirs. This was shown by the authors in previous studies where they separately quantified the impacts of dams on the riverine fluxes of N, P, and Si (Akbarzadeh et al., 2019; Maavara et al., 2014; Maavara, Parsons, et al., 2015). For example, their results indicated that in year 2000 existing dam reservoirs on average removed 21% of reactive Si (RSi = dissolved Si [DSi] + amorphous Si [ASi]), 43% of reactive P (RP = total dissolved P [TDP] + reactive particulate P [RPP]), and 35.5% of total N (TN). The model-predicted trend of preferential removal of RP over TN has been observed for a variety of individual dams (Bartoszek & Koszelnik, 2016; Donald et al., 2015; Garnier et al., 1999; Grantz et al., 2014; Maavara, Hood, et al., 2015; Maranger et al., 2018). In this study, we combine previous single-nutrient models to assess how existing and planned dams modify the TN:RP:RSi ratios delivered by rivers to coastal areas, taking into consideration the differential removal efficiencies of the three nutrient elements in reservoirs.

2. Materials and Methods

The in-reservoir biogeochemical cycles of N, P, and Si are each represented by a mechanistic mass balance model describing nutrient influxes, transformations, removal, and effluxes (Figure S1 and Table S1 in the supporting information). For RSi and RP the removal mechanism is burial with sediments accumulating in the reservoir. In addition to burial, TN is removed by denitrification. The reservoir nutrient removal efficiency, R_X , is defined as

$$R_X = \frac{X_{in} - X_{out}}{X_{in}} \times 100\%, \quad (1)$$

where X_{in} is the flux of RSi, RP or TN delivered to the reservoir via river inflow (mol year $^{-1}$), and X_{out} is the corresponding flux exiting the reservoir via the dam(s) (mol year $^{-1}$). For TN, N fixation is not included in X_{in} , because R_{TN} represents the net difference in the riverine TN fluxes entering and leaving the reservoir. That is, N fixation is treated as an in-reservoir process and is calculated for each reservoir independently based on the extent to which the river inflow is N-limited relative to P. Thus, for reservoirs receiving strongly N-limited river inflow, X_{out} may actually exceed X_{in} because of N fixation. The

reservoir then acts as a source of TN to the river system (Akbarzadeh et al., 2019, and references therein). For detailed descriptions of the mass balance models used to estimate removal of nutrient elements in dam reservoirs, see Maavara et al. (2014) for RSi, Maavara, Parsons, et al. (2015) for RP, and Akbarzadeh et al. (2019) for TN.

In-reservoir biotic and abiotic nutrient transformation and removal processes are represented by linear or saturation kinetic equations. The parameters in these equations (Table S1), as well as those describing the reservoirs' hydraulics and nutrient inputs, are assigned probability density functions (PDFs) that are derived from extensive reviews of the literature. Next, a large set of virtual dam reservoirs is generated by Monte Carlo simulations in which parameter values are repeatedly selected from the PDFs. Assuming that the nutrient dynamics in the set of virtual reservoirs are statistically representative of those of the world's real reservoirs, global relationships are extracted to describe water column nutrient removal as functions of τ_r (years) and inflowing nutrient fluxes (mol year^{-1}). In the case of N and P, the best fit equations (i.e., highest statistically significant R^2) for removal follow asymptotic relationships, while RSi removal is best represented with a power law. These relationships are combined with the watershed yields of RP, TN, and RSi extracted from the Global-NEWS model (Beusen et al., 2009; Mayorga et al., 2010) and then applied to the GRanD database of existing dams (Lehner et al., 2011), and that of hydroelectric dams under construction or planned (Zarfl et al., 2015).

One modification to the single-nutrient model calculations published previously is to account for the possibility of either P or N limitation of in-reservoir primary production, P_{pp} , according to

$$P_{pp} = P_{max} \frac{[nut]}{[nut] + K_{s,nut}}, \quad (2)$$

where P_{pp} is the photosynthetic fixation of either P or N (mol year^{-1}); $[nut]$ is the in-reservoir concentration (mol km^{-3}) of total dissolved P (TDP) or dissolved inorganic N (DIN), depending on whether primary production is P or N limited; $K_{s,nut}$ is the half-saturation rate constant of TDP or DIN (mol km^{-3}); and P_{max} is the maximum rate of primary productivity. The value of P_{max} varies with the reservoir's geographical location and is calculated as a function of the maximum photosynthetically active radiation (PAR), light extinction coefficient, metabolic index, maximum chl-a fixation rate, water temperature, number of ice-free days, and hours of daylight (for details, see Maavara et al., 2017). Thus, P_{max} represents the maximum annual photosynthetic production possible given the reservoir's light regime. Under low light availability, photosynthesis will be limited by the corresponding low value of P_{max} , irrespective of nutrient stoichiometry.

Note that P_{pp} and P_{max} are typically expressed in units of mass carbon (C) fixed per unit time. To convert between C, N, and P based photosynthetic rates, we assume that in-reservoir primary production follows the Redfield ratio, C:N:P = 106:16:1. At each time step, both the P and N models are run and the resulting in-reservoir molar DIN:TDP computed. If DIN:TDP < 16:1, the reservoir is assumed to be N limited, and $[nut] = \text{DIN}$ in Equation 2 during the next time step. If DIN:TDP \geq 16:1, the reservoir is assumed to be P limited, and $[nut] = \text{TDP}$. In-reservoir Si uptake by siliceous phytoplankton is a function of the RSi influx into the reservoir (Maavara et al., 2014), with the added condition that total Si uptake (expressed in mol Si year^{-1}) cannot exceed 100% of in-reservoir primary production.

For all river basin containing dams, parallel simulations with and without the dams are carried out. For the 1970 and 2000 calculations, we use the dams in the Global Reservoirs and Dams (GRanD) database (Lehner et al., 2011) that were in existence in those years, and the Global-NEWS nutrient yields for 1970 and 2000 (Mayorga et al., 2010). GRanD includes nearly 7,000 dams of all types (hydroelectric, storage, irrigation, etc.) and is the most complete spatially explicit dam database that is aligned to an existing drainage network data product, in this case, STN-30p (Vörösmarty et al., 2000). GRanD comprises nearly all reservoirs $>10 \text{ km}^2$ and includes reservoirs down to 0.1 km^2 .

The year 2030 and 2050 estimations include the GRanD dams plus the 3,000 + new hydroelectric dams cataloged by Zarfl et al. (2015). The latter database reflects the worldwide trend to prioritize construction of hydroelectric dams as an alternative energy source. Thus, while additional dams are certainly being built, we assume that our calculations account for the largest and most significant wave of ongoing and

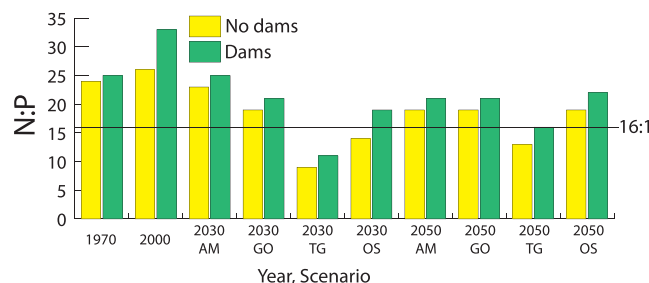


Figure 1. Global molar TN:RP ratios of river water delivered to the coastal zone using the nutrient loading yields of Global-NEWS for the four time points and the Millennium Assessment Scenarios: Adapting Mosaic (AM), Global Orchestration (GO), TechnoGarden (TG), and Order from Strength (OS). Results from the no-dam model calculations are in yellow; those including N and P processing in dam reservoirs are in green. The 16:1 line corresponds to the Redfield N:P ratio. The no-dam ratios only account for the variations in N and P inputs to rivers, while the with-dam ratios additionally account for the changing number and age distribution of dams in existence in 1970 and 2000, plus those of dams under construction or planned in 2030 and 2050.

the Global-NEWS year 2000 values are applied. For all scenarios and time points, we remove the Global-NEWS built-in dam correction factors and replace them by our reservoir-specific nutrient removal efficiencies for the dams reported in GRanD and Zarfl et al. (2015).

The nutrient discharges of the exorheic river basins that drain into the same marginal sea basin or shelf section are combined together. This is done by spatially intersecting the outlets of the STN-30p drainage networks (Vörösmarty et al., 2000) with the COSCAT/MARCAT segmentation of the continental margins (Laruelle et al., 2013) and applying a 0.5° buffer zone around the shelves to ensure overlap with the coarser STN-30p data set. For each coastal segment, the incoming riverine nutrient loads are summed and the nutrient ratios TN:RP, RSi:TN, and RSi:RP calculated for each time point. We note that the reported riverine nutrient loads and ratios do not account for modifications due to nutrient transformation and removal processes in the coastal zone, and for additional inputs from atmospheric deposition, coastal upwelling, or submarine groundwater discharge.

3. Results and Discussion

Dams increase the global TN:RP ratio delivered to the coastal zone because, on average, reservoirs remove P more efficiently than N (Figure 1). From 1970 to 2000, both the relative change in the anthropogenic loadings of N and P to rivers and the increasing number of dams contributed to the rising global riverine TN:RP ratio, a trend consistent with worldwide observations (Glibert, 2017; Tilman, 1999; Turner et al., 2003). However, this upward trend is projected to reverse resulting in lower TN:RP ratios in 2030 and 2050. The decrease of TN:RP ratios reflects the more effective control of N emissions, relative to P, assumed in the MEA scenarios. Although the ongoing boom in hydroelectric dam construction somewhat counteracts the drop in TN:RP, the effect of dams is smaller than for year 2000 because of the relatively short τ_r of the new dams.

The model simulations predict a general trend in TN:RP ratio from 2000 to 2030 (and 2050) that brings values closer to the Redfield ratio of marine phytoplankton (Figure 1). In itself, this would promote greater N limitation of coastal productivity in the coming decades. The projected trend, however, is a direct consequence of the assumptions underlying the MEA trajectories of land cover and land use change, human nutrient usage, and management. For example, the TG scenario yields the lowest TN:RP ratios for 2030 and 2050 (Figure 1), because this scenario assumes better N use efficiency through greater integration of livestock and crop production, as well as enhanced N removal in wastewater treatment and increasing P loads from manure application (Seitzinger et al., 2010). Nutrient loading and damming trajectories, however, are modulated by a large number of environmental, social, financial, and political drivers. Projections in riverine N and P fluxes and the associated TN:RP ratios therefore primarily inform about the consequences of decisions and

near-future river damming. The 2030 and 2050 estimates are further based on the RP and TN yields from the Millennium Ecosystem Assessment (MEA) scenarios in Global-NEWS (Seitzinger et al., 2010). We use the Global-NEWS MEA scenarios because they remain the only existing global scenarios for which spatially explicit nutrient loads to river systems are available.

The MEA scenarios capture a range of plausible future socioeconomic and environmental trajectories, specifically whether the world becomes more globalized (Global Orchestration [GO] and TechnoGarden [TG] scenarios) or regionalized (Order from Strength [OS] and Adapting Mosaic [AM] scenarios), and whether regions take a proactive (AM and TG) or reactive (GO and OS) approach to environmental change. Seitzinger et al. (2010) interpreted these scenarios to predict watershed-specific N and P loads using the Global-NEWS model for years 2030 and 2050, based on regional drivers such as fertilizer use efficiency, manure application, sewage treatment and effluent quality, crop-specific N fixation, and atmospheric N deposition (for additional details, see Bouwman et al., 2009; Fekete et al., 2010; and Van Drecht et al., 2009).

Because no corresponding RSi yields are available for 2030 and 2050,

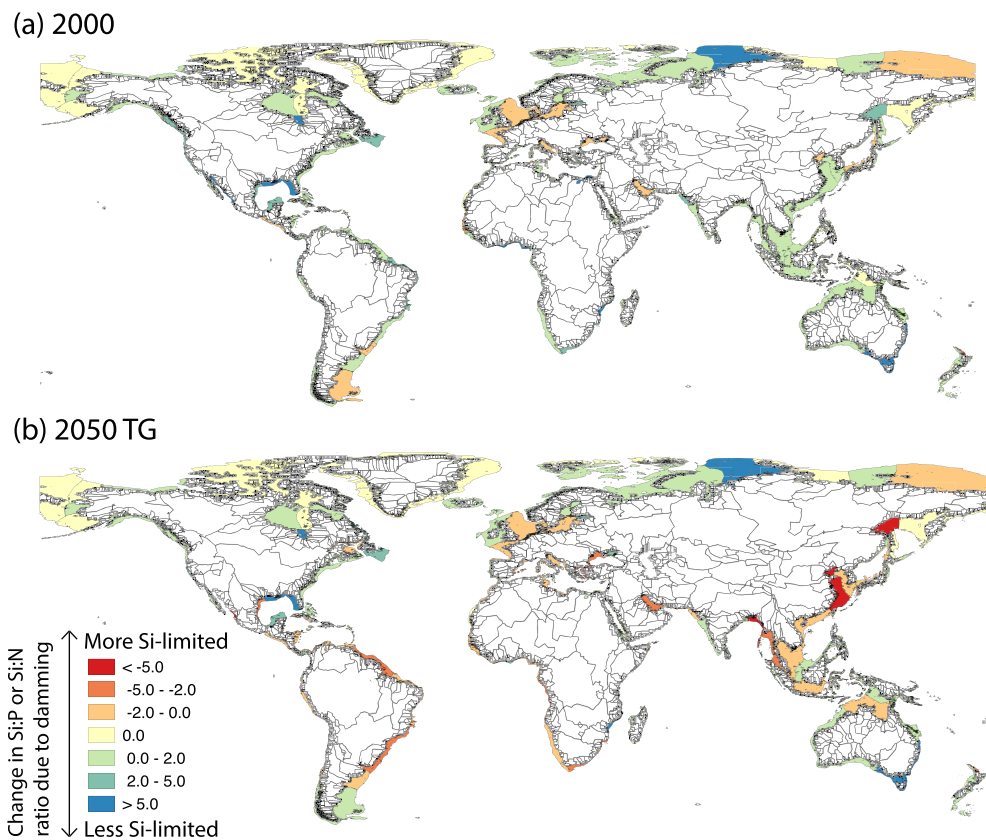


Figure 2. Effect of dams on riverine RSi:TN or RSi:RP ratios delivered to the world's coastal zones in (a) year 2000 and (b) year 2050 under the TechnoGarden (TG) scenario. The colors indicate whether the predicted RSi:TN or RSi:TP ratios increase (less Si limitation) or decrease (more Si limitation) relative to the calculations where the effects of damming are removed. The changes in RSi:TN values are multiplied by 16 to be comparable with changes in RSi:RP ratios. The TG scenario yields the largest changes in TN:RP ratios and the largest differences in the RSi:TN and RSi:RP ratios between the calculations with and without dams. Nutrient ratios for all scenarios and time points are given in Data Set S1.

circumstances that may, or may not, come to pass. They can obviously not account for unpredictable events, conditions and actions not considered in the scenarios.

The global average TN:RP ratios mask the high geographical variability of the nutrient ratios discharged by rivers into the coastal ocean (Data Set S1). This is also true for the effect of damming on these nutrient ratios. For instance, for year 2000 a molar TN:RP ratio of 36 is estimated for the total river outflow to the northern shelf of the East China Sea, including from the Yangtze and Huai Rivers. Without the dams, the model-derived TN:RP ratio would be 29; that is, the presence of dams increases the TN:RP ratio by 24%. Damming may therefore be an important driver of the enhanced P limitation of coastal primary production observed in the East China Sea (Wang et al., 2003; Wong et al., 1998), further implying that efforts to reduce anthropogenic N loads to mitigate coastal eutrophication may be partly offset by the extensive dam construction in the contributing watersheds. The watersheds draining into the Bay of Bengal, Andaman Sea, and regions around the Malay Peninsula, including the Mekong, Ganges-Brahmaputra, and Irrawaddy, also represent major hotspots of dam construction (Data Set S1, Figure 2). The impact of dams is especially significant for the Mekong River discharge: Without dams the TN:RP ratios for all 2050 scenarios are close to the Redfield value, with the new dams the ratios move toward or into P limitation.

Results for years 1970 and 2000 imply that damming increased the RSi:TN and RSi:RP ratios in most of the world's river systems because, on average, reservoirs preferentially eliminate RP and TN over RSi. In 2000, for example, dams eliminated on average 21% of inflowing RSi, 43% of RP, and 35.5% of TN. In other words, while dams globally reduce the absolute river discharge of RSi (Humborg et al., 2000), they also help to

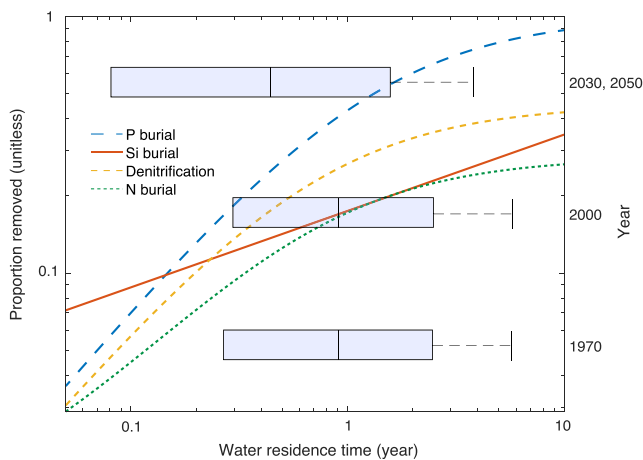


Figure 3. Primary y axis: the average proportions of RP, TN, and RSi eliminated by reservoirs as a function of the water residence time (years), via burial for all three nutrients, plus denitrification. Secondary y axis: time points for the global distributions of reservoir water residence times. Box edges indicate standard deviations, the line inside the box is the median, and upper whiskers are third quartiles. Outliers are not shown for clarity, but none fell below the lower standard deviation. All equations are asymptotic functions except RSi burial, which is a power law function. Derivations can be found in Maavara et al. (2014), Akbarzadeh et al. (2019), and Maavara, Parsons, et al. (2015).

global changes, in conjunction with river damming, will be crucial for predicting coastal changes to RSi:TN and RSi:RP ratios.

The trend in Figure 2 reflects the typically low τ_r of the new hydroelectric dams. The global nutrient removal relationships we derived predict that when τ_r drops below ~50 days, though all nutrient removal efficiencies decrease, the RSi removal efficiency in reservoirs exceeds those of TN and RP (Figure 3). This is consistent with the competitive ability of diatoms to establish communities more rapidly than other phytoplankton species (Hall et al., 1999; Paerl et al., 2006), especially in turbulent, light-limited environments characteristic of high-discharge hydroelectric reservoirs (Huisman et al., 2004). A short τ_r also limits how much particulate RSi can dissolve and be exported as DSi from the reservoir. As a consequence, while in year 2000 dams increased the RSi:RP ratio in 87% of P-limited river discharge to the coastal zone and in 98% of N-limited river discharge, by midcentury around 60% of riverine discharge worldwide would experience decreasing RSi:RP and RSi:TN ratios because of the newly constructed dams (Figure 2; Data Set S1).

Most dams under construction or planned are hydroelectric dams that rely on passing high volumes of water through their turbines over short timeframes (Zarfl et al., 2015). Thus, globally, these new dams are causing a drop in the mean τ_r of dam reservoirs (Figure 3). In contrast, during the first boom in dam construction following World War II, the focus was on building large storage dams with longer τ_r . In 1970 and 2000, only 10% and 16% of the dam reservoirs included in our analysis have τ_r below 50 days, respectively (Lehner et al., 2011). The new hydroelectric dams would raise this to 32% by 2030.

The predicted shift toward shorter τ_r in the coming decades and the associated changes in riverine RSi:TN and RSi:RP ratios assume that the dams in (Zarfl et al., 2015) are representative of all the dams that will come into existence in the near future. This assumption will be difficult to verify without further expansion of the current databases on dams and their reservoirs, as well as the acquisition of more data on nutrient fluxes and speciation upstream and downstream of existing and newly built reservoirs. The application of new monitoring technologies, including remote sensing and machine learning, may enable a more systematic surveying of reservoirs, which is required to fully assess their potential global environmental impacts.

The predicted increase in Si-limited river discharge to the coastal zone in years 2030 and 2050 will take place primarily in Southeast Asia, South America, and Africa (Figure 2; Data Set S1), that is, regions that are experiencing both some of the fastest dam construction activities and largest increases in anthropogenic

buffer the impact on coastal siliceous communities by reducing the supplies of TN and RP even more, at least until the turn of the century. Nonetheless, dams have not been able to completely balance the rapid increases in anthropogenic TN and RP loadings, relative to RSi loading. Hence, RSi:TN and RSi:RP ratios in rivers reaching the sea have generally experienced significant declines.

The model results further suggest that we may be at a turning point where the massive construction of hydroelectric dams may actually reverse the effect of dams on the RSi:TN and RSi:RP ratios. This is illustrated in Figure 2, which shows which of the world's coastal segments the presence of dams in the contributing watersheds increases or decreases the discharge of RSi relative to that of RP or TN. Note that RSi:TN is used for segments where TN:RP < 16 (N-limited river discharge) and RSi:RP ratio where TN:RP \geq 16 (P-limited river discharge). As can be seen, compared to year 2000, the 2050 TG scenario predicts significantly more coastal segments where damming decreases the riverine RSi:TN or RSi:RP ratio. These impacts will undoubtedly be further modified by future land use and land cover changes to RSi loads to rivers for which, unfortunately, we do not have spatially explicit scenarios (in contrast to the RP and TN loads). For example, Carey and Fulweiler (2012) showed that with reforestation or conversion to agricultural land use, Si loads decrease due to plant Si uptake and repeated harvest, while urbanization increases Si loads from wastewater effluents. Given their estimate that land use and land cover variables drive 40–70% of the Si loads to the oceans, quantification of these

macronutrient loading, in particular of P. An example of a hot spot of dam construction and rapid environmental change is the Yangtze River basin where over 50,000 dams have already been built and an additional 142 large hydroelectric dams are planned or under construction (Yang et al., 2011; Zarfl et al., 2015). The TG scenario predicts a moderate growth in P loading due partially to rising manure applications, compared with a lesser increase in N loads due to rising fertilizer N use efficiency (Seitzinger et al., 2010). Consequently, between 2000 and 2050 the molar TN:RP ratio discharged to the coast would drop from 36 to 8, strongly promoting N-limitation in the Yangtze River estuary and adjacent nearshore marine environment. In addition, the growing difference in RSi and TN removal efficiencies by dams may lead to a decrease in the RSi:TN ratio. Our results imply that by 2050 the RSi:TN ratio in the Yangtze River discharge may drop to 0.74, that is, below the Redfield Si:N ratio, compared to 1.45 when dams are excluded from the calculations. For the Ganges-Brahmaputra Rivers, all 2050 scenarios predict that damming will take slightly Si-limited discharge (RSi:TN = 0.60–0.72) into severe Si limitation (RSi:TN = 0.17–0.19), due to the construction of more than 400 new dams.

Because dams generally reduce the riverine flows of N, P, and Si, they may be seen as benefitting downstream coastal areas by mitigating the threat of eutrophication. However, as shown here, the role of dams in nutrient delivery to the coastal zone not only varies among the different macronutrient elements but also changes over time, with ecological consequences that are far from fully understood. Furthermore, while damming may help reduce nutrient enrichment of the receiving coastal areas, this comes at the expense of eutrophication in the rivers and dam reservoirs themselves. In addition, our results suggest that we may have reached a turning point in how dams modify riverine nutrient ratios, because of the current emphasis on building high-throughput hydroelectric dams. The latter, together with an anticipated disproportionate growth of anthropogenic P loading to rivers, could result in dams becoming increasingly less efficient at attenuating N and Si limitation of coastal productivity.

Data Availability Statement

Modeled TN:RP:RSi ratios for coastal zones worldwide are included in Data Set S1, which is archived in HydroShare (at the URL <http://www.hydroshare.org/resource/aa2a766e93814da68147272f65a007b6>)

Acknowledgments

This research was funded by the Natural Sciences and Engineering Research Council of Canada (NSERC), Award PDF-516575-2018, and Canada Excellence Research Chair Program (CERC).

References

- Akbarzadeh, Z., Maavara, T., Slowinski, S., & Van Cappellen, P. (2019). Effects of damming on river nitrogen fluxes: A global analysis. *Global Biogeochemical Cycles*, 33, 1339–1357. <https://doi.org/10.1029/2019GB006222>
- Bartoszek, L., & Koszelnik, P. (2016). The qualitative and quantitative analysis of the coupled C, N, P and Si retention in complex of water reservoirs. *Springerplus*, 5, 1157. <https://doi.org/10.1186/s40064-016-2836-7>
- Bates, S. S., Hubbard, K. A., Lundholm, N., Montresor, M., & Leaw, C. P. (2018). Pseudo-nitzschia, Nitzschia, and domoic acid: New research since 2011. *Harmful Algae*, 79, 3–43. <https://doi.org/10.1016/j.hal.2018.06.001>
- Beusen, A., Bouwman, A., Dürr, H., Dekkers, A., & Hartmann, J. (2009). Global patterns of dissolved silica export to the coastal zone: Results from a spatially explicit global model. *Global Biogeochemical Cycles*, 23, GB0A02. <https://doi.org/10.1029/2008GB003281>
- Billen, G., & Garnier, J. (2007). River basin nutrient delivery to the coastal sea: Assessing its potential to sustain new production of non-siliceous algae. *Marine Chemistry*, 106, 148–160. <https://doi.org/10.1016/j.marchem.2006.12.017>
- Billen, G., Lancelot, C., Meybeck, M., Mantoura, R., Martin, J.-M., & Wollast, R. (1991). *N, P and Si retention along the aquatic continuum from land to ocean, ocean margin processes in global change*, 1 (pp. 19–44). Chichester, UK: John Wiley & Sons.
- Bouwman, A., Beusen, A. H., & Billen, G. (2009). Human alteration of the global nitrogen and phosphorus soil balances for the period 1970–2050. *Global Biogeochemical Cycles*, 23, GB0A04. <https://doi.org/10.1029/2009GB003576>
- Brett, M., & Müller-Navarra, D. (1997). The role of highly unsaturated fatty acids in aquatic foodweb processes. *Freshwater Biology*, 38(3), 483–499. <https://doi.org/10.1046/j.1365-2427.1997.00220.x>
- Brzezinski, M. (1985). The Si: C: N ratio of marine diatoms: Interspecific variability and the effect of some environmental variables. *Journal of Phycology*, 21, 347–357.
- Buchan, A., LeClerc, G. R., Gulvik, C. A., & González, J. M. (2014). Master recyclers: Features and functions of bacteria associated with phytoplankton blooms. *Nature Reviews Microbiology*, 12, 686–698. <https://doi.org/10.1038/nrmicro3326>
- Carey, J. C., & Fulweiler, R. (2012). Human activities directly alter watershed dissolved silica fluxes. *Biogeochemistry*, 111, 125–138. <https://doi.org/10.1007/s10533-011-9671-2>
- Compton, J., Mallinson, D., Glenn, C., Filippelli, G., Föllmi, K., Shields, G., & Zanin, Y. (2000). Variations in the global phosphorus cycle. *Marine Authigenesis: From Global to Microbial; SEPM Special Publication*, 66, 21–33.
- Donald, D. B., Parker, B. R., Davies, J.-M., & Leavitt, P. R. (2015). Nutrient sequestration in the Lake Winnipeg watershed. *Journal of Great Lakes Research*, 41, 630–642. <https://doi.org/10.1016/j.jglr.2015.03.007>
- Falkowski, P. G., Barber, R. T., & Smetacek, V. (1998). Biogeochemical controls and feedbacks on ocean primary production. *Science*, 281(5374), 200–206. <https://doi.org/10.1126/science.281.5374.200>
- Fekete, B. M., Wisser, D., Kroese, C., Mayorga, E., Bouwman, L., Wollheim, W. M., & Vörösmarty, C. (2010). Millennium ecosystem assessment scenario drivers (1970–2050): Climate and hydrological alterations. *Global Biogeochemical Cycles*, 24, GB0A12. <https://doi.org/10.1029/2009GB003593>

- Filippelli, G. M. (2008). The global phosphorus cycle: Past, present, and future. *Elements*, 4, 89–95. <https://doi.org/10.2113/GSELEMENTS.4.2.89>
- Friedl, G., & Wüest, A. (2002). Disrupting biogeochemical cycles—Consequences of damming. *Aquatic Sciences*, 64(1), 55–65. <https://doi.org/10.1007/s00027-002-8054-0>
- Galloway, J. N., Dentener, F. J., Capone, D. G., Boyer, E. W., Howarth, R. W., Seitzinger, S. P., et al. (2004). Nitrogen cycles: Past, present, and future. *Biogeochemistry*, 70, 153–226. <https://doi.org/10.1007/s10533-004-0370-0>
- Garnier, J., Beusen, A., Thieu, V., Billen, G., & Bouwman, L. (2010). N: P: Si nutrient export ratios and ecological consequences in coastal seas evaluated by the ICEP approach. *Global Biogeochemical Cycles*, 24, GB0A05. <https://doi.org/10.1029/2009GB003583>
- Garnier, J., Leporeq, B., Sanchez, N., & Philippon, X. (1999). Biogeochemical mass-balances (C, N, P, Si) in three large reservoirs of the Seine Basin (France). *Biogeochemistry*, 47, 119–146. <https://doi.org/10.1007/bf00994919>
- Glibert, P. M. (2017). Eutrophication, harmful algae and biodiversity—Challenging paradigms in a world of complex nutrient changes. *Marine Pollution Bulletin*, 124(2), 591–606. <https://doi.org/10.1016/j.marpolbul.2017.04.027>
- Gong, G. C., Chang, J., Chiang, K. P., Hsiung, T. M., Hung, C. C., Duan, S. W., & Codispoti, L. (2006). Reduction of primary production and changing of nutrient ratio in the East China Sea: Effect of the Three Gorges Dam? *Geophysical Research Letters*, 33, L07610. <https://doi.org/10.1029/2006GL025800>
- Grantz, E. M., Haggard, B. E., & Scott, J. T. (2014). Stoichiometric imbalance in rates of nitrogen and phosphorus retention, storage, and recycling can perpetuate nitrogen deficiency in highly-productive reservoirs. *Limnology and Oceanography*, 59, 2203–2216. <https://doi.org/10.4319/lo.2014.59.6.2203>
- Grill, G., Lehner, B., Lumsdon, A. E., MacDonald, G. K., Zarfl, C., & Liermann, C. R. (2015). An index-based framework for assessing patterns and trends in river fragmentation and flow regulation by global dams at multiple scales. *Environmental Research Letters*, 10, 015001. <https://doi.org/10.1088/1748-9326/10/1/015001>
- Grill, G., Lehner, B., Thieme, M., Geenen, B., Tickner, D., Antonelli, F., et al. (2019). Mapping the world's free-flowing rivers. *Nature*, 569, 215–221. <https://doi.org/10.1038/s41586-019-1111-9>
- Hall, R. I., Smol, J. P., & Smol, J. (1999). Diatoms as indicators of lake eutrophication. *The diatoms: applications for the environmental and earth sciences*, 128–168. <https://doi.org/10.1017/CBO9780511613005.007>
- Huisman, J., Sharples, J., Stroom, J. M., Visser, P. M., Kardinaal, W. E. A., Verspagen, J. M., & Sommeijer, B. (2004). Changes in turbulent mixing shift competition for light between phytoplankton species. *Ecology*, 85, 2960–2970. <https://doi.org/10.1890/03-0763>
- Humborg, C., Conley, D. J., Rahm, L., Wulff, F., Cociasu, A., & Ittekkot, V. (2000). Silicon retention in river basins: Far-reaching effects on biogeochemistry and aquatic food webs in coastal marine environments. *Ambio: A Journal of the Human Environment*, 29(1), 45–50. <https://doi.org/10.1579/0044-7447-29.1.45>
- Humborg, C., Pastuszak, M., Aigars, J., Siegmund, H., Mörtb, C.-M., & Ittekkot, V. (2006). Decreased silica land-sea fluxes through damming in the Baltic Sea catchment—Significance of particle trapping and hydrological alterations. *Biogeochemistry*, 77, 265–281. <https://doi.org/10.1007/s10533-005-1533-3>
- Laruelle, G. G., Durr, H. H., Lauerwald, R., Hartmann, J., Slomp, C. P., Goossens, N., & Regnier, P. A. G. (2013). Global multi-scale segmentation of continental and coastal waters from the watersheds to the continental margins. *Hydrology and Earth System Sciences*, 17, 2029–2051. <https://doi.org/10.5194/hess-17-2029-2013>
- Lehner, B., Liermann, C. R., Revenga, C., Vörösmarty, C., Fekete, B., Crouzet, P., et al. (2011). High-resolution mapping of the world's reservoirs and dams for sustainable river-flow management. *Frontiers in Ecology and the Environment*, 9, 494–502. <https://doi.org/10.1890/100125>
- Maavara, T., Chen, Q., Van Meter, K., Brown, L. E., Zhang, J., Ni, J., & Zarfl, C. (2020). River dam impacts on biogeochemical cycling. *Nature Reviews Earth & Environment*, 1, 103–116. <https://doi.org/10.1038/s43017-019-0019-0>
- Maavara, T., Dürr, H. H., & Van Cappellen, P. (2014). Worldwide retention of nutrient silicon by river damming: From sparse data set to global estimate. *Global Biogeochemical Cycles*, 28, 842–855. <https://doi.org/10.1002/2014GB004875>
- Maavara, T., Hood, J. L. A., North, R. L., Doig, L. E., Parsons, C. T., Johansson, J., et al. (2015). Reactive silicon dynamics in a large prairie reservoir (Lake Diefenbaker, Saskatchewan). *Journal of Great Lakes Research*, 41, 100–109. <https://doi.org/10.1016/j.jglr.2015.04.003>
- Maavara, T., Lauerwald, R., Regnier, P., & Van Cappellen, P. (2017). Global perturbation of organic carbon cycling by river damming. *Nature Communications*, 8, 15347. <https://doi.org/10.1038/ncomms15347>
- Maavara, T., Parsons, C. T., Ridenour, C., Stojanovic, S., Dürr, H. H., Powley, H. R., & Van Cappellen, P. (2015). Global phosphorus retention by river damming. *Proceedings of the National Academy of Sciences*, 112, 15,603–15,608. <https://doi.org/10.1073/pnas.1511797112>
- Mangas-Sánchez, J., & Adlercreutz, P. (2015). Highly efficient enzymatic biodiesel production promoted by particle-induced emulsification. *Biotechnology for Biofuels*, 8, 58. <https://doi.org/10.1186/s13068-015-0247-6>
- Maranger, R., Jones, S. E., & Cotner, J. B. (2018). Stoichiometry of carbon, nitrogen, and phosphorus through the freshwater pipe. *Limnology and Oceanography Letters*, 3, 89–101. <https://doi.org/10.1002/lol2.10080>
- Mayorga, E., Seitzinger, S. P., Harrison, J. A., Dumont, E., Beusen, A. H., Bouwman, A., et al. (2010). Global nutrient export from WaterSheds 2 (NEWS 2): Model development and implementation. *Environmental Modelling & Software*, 25, 837–853. <https://doi.org/10.1016/j.envsoft.2010.01.007>
- Officer, C., & Ryther, J. (1980). The possible importance of silicon in marine eutrophication. *Marine Ecology Progress Series*, 3, 83–91. <https://doi.org/10.3354/meps003083>
- Paerl, H. W., Valdes, L. M., Peierls, B. L., Adolf, J. E., & Lawrence, W. H. Jr. (2006). Anthropogenic and climatic influences on the eutrophication of large estuarine ecosystems. *Limnology and Oceanography*, 51, 448–462. https://doi.org/10.4319/lo.2006.51.1_part_2.0448
- Parsons, M., Scholin, C., Miller, P., Doucette, G., Powell, C., Fryxell, G., et al. (1999). Pseudo-nitzschia in Lousiana coastal waters: Molecular probe field trials, genetic variability, and domoic acid analyses. *Journal of Phycology*, 35(6), 1368–1378. <https://doi.org/10.1046/j.1529-8817.1999.3561368.x>
- Parsons, M. L., Dortch, Q., & Turner, R. E. (2002). Sedimentological evidence of an increase in Pseudo-nitzschia (Bacillariophyceae) abundance in response to coastal eutrophication. *Limnology and Oceanography*, 47(2), 551–558. <https://doi.org/10.4319/lo.2002.47.2.00551>
- Redfield, A. (1934). On the proportions of organic derivatives in sea water and their relation to the composition of plankton. *James Johnstone Memorial Volume* (pp. 177–192). Liverpool, UK: University Press of Liverpool.
- Royer, T. V. (2020). Stoichiometry of nitrogen, phosphorus, and silica loads in the Mississippi-Atchafalaya River basin reveals spatial and temporal patterns in risk for cyanobacterial blooms. *Limnology and Oceanography*, 65, 325–335. <https://doi.org/10.1002/lnco.11300>

- Seitzinger, S., Mayorga, E., Bouwman, A., Kroese, C., Beusen, A., Billen, G., et al. (2010). Global river nutrient export: A scenario analysis of past and future trends. *Global Biogeochemical Cycles*, 24, GB0A08. <https://doi.org/10.1029/2009GB003587>
- Strokal, M., Yang, H., Zhang, Y., Kroese, C., Li, L., Luan, S., et al. (2014). Increasing eutrophication in the coastal seas of China from 1970 to 2050. *Marine Pollution Bulletin*, 85(1), 123–140. <https://doi.org/10.1016/j.marpolbul.2014.06.011>
- Struyf, E., Smis, A., Van Damme, S., Garnier, J., Govers, G., Van Wesemael, B., et al. (2010). Historical land use change has lowered terrestrial silica mobilization. *Nature Communications*, 1, 129. <https://doi.org/10.1038/ncomms1128>
- Tilman, D. (1999). Global environmental impacts of agricultural expansion: The need for sustainable and efficient practices. *Proceedings of the National Academy of Sciences*, 96(11), 5995–6000. <https://doi.org/10.1073/pnas.96.11.5995>
- Turner, R., Rabalais, N., Justic, D., & Dortch, Q. (2003). Global patterns of dissolved N, P and Si in large rivers. *Biogeochemistry*, 64(3), 297–317. <https://doi.org/10.1023/A:1024960007569>
- Van Drecht, G., Bouwman, A., Harrison, J., & Knoop, J. (2009). Global nitrogen and phosphate in urban wastewater for the period 1970 to 2050. *Global Biogeochemical Cycles*, 23, GB0A03. <https://doi.org/10.1029/2009gb003458>
- Vandevenne, F., Struyf, E., Clymans, W., & Meire, P. (2012). Agricultural silica harvest: Have humans created a new loop in the global silica cycle? *Frontiers in Ecology and the Environment*, 10, 243–248. <https://doi.org/10.1890/110046>
- Vitousek, P. M., Aber, J. D., Howarth, R. W., Likens, G. E., Matson, P. A., Schindler, D. W., et al. (1997). Human alteration of the global nitrogen cycle: Sources and consequences. *Ecological Applications*, 7, 737–750. [https://doi.org/10.1890/1051-0761\(1997\)007\[0737:haotgn\]2.0.co;2](https://doi.org/10.1890/1051-0761(1997)007[0737:haotgn]2.0.co;2)
- Vörösmarty, C., Fekete, B., Meybeck, M., & Lammers, R. (2000). Geomorphometric attributes of the global system of rivers at 30-minute spatial resolution. *Journal of Hydrology*, 237(1-2), 17–39. [https://doi.org/10.1016/S0022-1694\(00\)00282-1](https://doi.org/10.1016/S0022-1694(00)00282-1)
- Vorosmarty, C., Sharma, K., Fekete, B. M., Copeland, A., Holden, J., Marble, J., & Lough, J. (1997). The storage and aging of continental runoff in large reservoir systems of the world. *Ambio*, 26, 210–219.
- Wang, B.-D., Wang, X.-L., & Zhan, R. (2003). Nutrient conditions in the Yellow Sea and the East China Sea. *Estuarine, Coastal and Shelf Science*, 58(1), 127–136. [https://doi.org/10.1016/S0272-7714\(03\)00067-2](https://doi.org/10.1016/S0272-7714(03)00067-2)
- Wong, G., Gong, G., Liu, K., & Pai, S. (1998). “Excess nitrate” in the East China Sea. *Estuarine, Coastal and Shelf Science*, 46(3), 411–418. <https://doi.org/10.1006/ecss.1997.0287>
- Yang, S., Milliman, J., Li, P., & Xu, K. (2011). 50,000 dams later: Erosion of the Yangtze River and its delta. *Global and Planetary Change*, 75, 14–20. <https://doi.org/10.1016/j.gloplacha.2010.09.006>
- Zarfl, C., Lumsdon, A., Berlekamp, J., Tydecks, L., & Tockner, K. (2015). A global boom in hydropower dam construction. *Aquatic Sciences*, 77, 161–170. <https://doi.org/10.1007/s00027-014-0377-0>